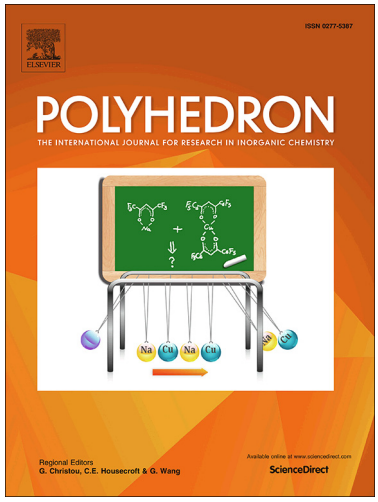

Synthesis, characterization and X-ray crystal structure of potentially N_6O_2 co-ordinating macroacyclic Schiff base ligands and their Mn(II), Zn(II) and Cd(II) complexes; cytotoxic, antibacterial properties and competitive ^{7}Li NMR studies

Fatemeh Forouzandeh, Hassan Keypour, Mohammad Hasan Zebarjadian, Masoumeh Mahmoudabadi, Leila Hosseinzadeh, Roya Karamian, Masoumeh Ahmadi Khoei, Robert William Gable

PII: S0277-5387(19)30004-X
DOI: https://doi.org/10.1016/j.poly.2018.12.052
Reference: POLY 13670

To appear in: *Polyhedron*

Received Date: 28 October 2018
Revised Date: 26 December 2018
Accepted Date: 29 December 2018

Please cite this article as: F. Forouzandeh, H. Keypour, M.H. Zebarjadian, M. Mahmoudabadi, L. Hosseinzadeh, R. Karamian, M.A. Khoei, R.W. Gable, Synthesis, characterization and X-ray crystal structure of potentially N_6O_2 coordinating macroacyclic Schiff base ligands and their Mn(II), Zn(II) and Cd(II) complexes; cytotoxic, antibacterial properties and competitive ^{7}Li NMR studies, *Polyhedron* (2019), doi: https://doi.org/10.1016/j.poly.2018.12.052

Synthesis, characterization and X-ray crystal structure of potentially N_6O_2 coordinating macroacyclic Schiff base ligands and their Mn(II), Zn(II) and Cd(II) complexes; cytotoxic, antibacterial properties and competitive ^7Li NMR studies

Fatemeh Forouzandeh[a], Hassan Keypour[a,*], Mohammad Hasan Zebarjadian[b], Masoumeh Mahmoudabadi[a], Leila Hosseinzadeh[c], Roya Karamian[d], Masoumeh Ahmadi Khoei[d], Robert William Gable[e]

[a] *Faculty of Chemistry, Bu-Ali Sina University, Hamedan 65174, Iran*

[b] *Farhangian University, Hamedan 6513666157, Iran*

[c] *Pharmaceutical Sciences Research Center, karmanshah University of Medical Sciences, Kermanshah, Iran*

[d] *Department of Biology, Bu-Ali Sina University, Hamedan 65175/4661, Iran*

[e] *School of Chemistry, University of Melbourne, Victoria 3010, Australia*

* Corresponding authors. Tel.+98 (81) 38242044; fax:+98 (81) 38272404.

E-mail addresses: haskey1@yahoo.com (H. Keypour).

Abstract

In this work, two new symmetrical, potentially N_6O_2 coordinating, macroacyclic Schiff base ligands (H_2L^1 and H_2L^2) were derived from the condensation of a newly synthesized polyamine, 2,2'-(ethane-1,2-diylbis(piperazine-4,1-diyl))bis(ethan-1-amine)(A),with 2-Hydroxybenzaldehyde and 2-hydroxy-3-methoxybenzaldhyde respectively. Six macroacylic Schiff base complexes were prepared by direct reaction of H_2L^1 or H_2L^2 with Mn(II), Zn(II) or Cd(II) metal ions in equimolar ratios. The products were characterized by several physicochemical measurements. As well, the crystal structure of H_2L^1 was confirmed by a single crystal X-ray structural analysis. Competitive ^{7}Li NMR experiments were used to probe the complexation of Mn^{2+}, Zn^{2+} and Cd^{2+} ions with (H_2L^1) and (H_2L^2) in both acetonitrile and methanol. The stabilities of the final complexes were found to be in the order M-(H_2L^1) > M-(H_2L^2) and Cd^{2+}> Zn^{2+}> Mn^{2+}. The cytotoxic and antibacterial properties of these complexes were also investigated.

Keywords: Macroacyclic Schiff base, Piperazine, Stoichiometry and stability of complexes, Cytotoxic, Antibacterial

1. Introduction

Schiff base complexes have remained the most important stereo chemical models in main group and transition metal coordination chemistry because of their structural variety and simplicity in their synthesis [1, 2]. They have an important role in many areas of coordination chemistry, from classic synthetic chemistry to modern biochemical and physicochemical studies of metal complexes [3-8]. Piperazine is one of the most extensively used and studied heterocyclic compounds. The piperazine moiety is a structural part of many analgesics, psychotropic and antitumor drugs [9-11]. It is a useful component in the design of both macroacyclic and macrocyclic compounds due to a number of structural properties, such as having a bifunctional scaffold for the linkers, acting as a good hydrogen-bond acceptor, having the ability to complex with a variety of metal ions and the capability of undergoing nucleophilic substitution reactions with different types of halide compounds [12]. As well, piperazine compounds have good potential for the development of new bioactive agents [13]. Accordingly, we have focused on the design and synthesis of new Schiff base ligands containing the piperazine moiety for several years. During last decade, we have reported a number of macrocyclic and macroacyclic Schiff base complexes containing one piperazine moiety with Zn(II), Mn(II) and Cd(II) metal ions [14-20]. In this work, we report the synthesis of Schiff base ligands bearing two piperazine moieties and their Zn(II), Mn(II) and Cd(II) complexes. These complexes were characterized by several physicochemical techniques and, in case of H_2L^1*, an X-ray structural analysis. Their cytotoxic and antibacterial properties have also been investigated.*

2. Experimental

2.1. Materials

1,2-dibromoethane, 1-(2-aminoethyl)piperazine, phthalic anhydride, 2-Hydroxybenzaldehyde, 2-Hydroxy-3-methoxybenzaldehyde and the manganese, zinc and cadmium perchlorates were commercial products (from Merck, Aldrich and Fluka), and were used without further purification. Solvents were of reagent grade and were purified by the usual methods.

Caution! Perchlorate salts are potentially explosive. Only a small amount of material should be prepared and handled with great care.

2.2. *Instrumentation*

CHN analyses were carried out using a Perkin–Elmer, CHNS/O elemental analyzer model 2400 series 2. Infrared spectra were measured using KBr pellets on a BIO-RADFTS-40A spectrophotometer (4000–400 cm^{-1}). ^{1}H and ^{13}C NMR spectra were measured in DMSO-d_6 and $CDCl_3$-d on a Bruker Avance 400 MHz spectrometer using $Si(CH_3)_4$ as an internal standard. Mass spectra were recorded on an Agilent technologies (HP) 5973 mass spectrometer operating at an ionization potential of 70 eV.

2.3. X-ray crystallography

Light yellow single crystals of H_2L^1 [$C_{28}H_{40}N_6O_2$] were crystallized by slow evaporation from methanol. Data collection was carried out on a Rigaku Oxford Diffraction SuperNova diffractometer using mirror monochromated Cu Kα radiation (λ = 1.54184 Å) at 130 K. Using Olex2 [21], the structure was solved with the ShelXT [22] structure solution program using Intrinsic Phasing and refined with the ShelXL [23] refinement package using Least Squares minimization on F^2, using all data. Gaussian absorption corrections were applied to the data. All non-hydrogen atoms were refined with anisotropic displacement parameters, while all hydrogen atoms were refined with isotropic displacement parameters. Crystallographic data for the ligand H_2L^1 is listed in Table 1.

<Please insert Table 1>

2.4. ^{7}Li NMR spectroscopy study

All NMR measurements were made using a Jeol 90Q FX-FT NMR spectrometer with a field strength of 2.113 Tesla. The temperature of the probe was fixed to ± 0.1°C using the temperature controller in the spectrometer. The lithium-7 NMR spectra of the solutions were recorded at 25.0(1) ºC. Under these conditions, lithium-7 resonates at 33.742 MHz. A 4.0 molar aqueous LiCl solution was used as external reference and the recorded lithium-7 chemical shifts refer to this solution; the upfield shift from the reference defined as negative. Stock solutions of the Schiff bases were prepared with concentrations of 0.1 M, in both methanol and acetonitrile, while solutions of the metal perchlorates, in both methanol and acetonitrile, were prepared at concentrations of 0.01 M. The solutions of the metal salts, in both solvents, were titrated against

the solutions of both Schiff bases, up to a ligand:metal mole ratio of 4. *Using a micro syringe, an aliquot of the Schiff base ligand was added to the solution of the metal and the resulting solution put in an ultrasonic stirrer for 10 minutes after which the solution was thermostated at 25 °C for 10 min to achieve temperature equilibrium.*

2.5. Synthesis

2.5.1. Synthesis of 2,2'-(ethane-1,2-diylbis(piperazine-4,1-diyl))bis(ethan-1-amine) (A)

Phthalic anhydride (1.48 g, 10 mmol) was melted in a beaker at 180 °C followed by the addition 1-(2-Aminoethyl)piperazine (1.29 g, 10 mmol) to the beaker and mixture stirred for 15 min, after which the mixture was then allowed to cool. The resulting solid was washed with hot ethanol and then dissolved in hot acetonitrile followed by the drop wise addition of 1,2-dibromoethane (0.94 g, 5 mmol) after which the solution refluxed for 48 hours. The solid product was then filtered off, extracted with chloroform and then refluxed with 25% aqueous HCl (300 ml) for 12 h. After cooling, the phthalic acid produced was filtered off and the solution evaporated to a small volume after which and the hexamine salt was precipitated by the addition of absolute ethanol and the solid washed with a small amount of diethyl ether. To a suspension of the amine salt (1 mmol) in ethanol (10 ml) was added a solution of NaOH (6 mmol) in ethanol (10 ml). The resulted mixture was stirred for 30 minutes at room temperature. The precipitate was filtered off and the filtrate evaporated to dryness. The resulting white powder was characterized as the pure compound (scheme 1). Yield: 0.85 g (60%). EI-MS (m/z): 284. IR (KBr, cm^{-1}): 3293–3443, 1628 $\nu(NH_2)$. ^1H NMR (D_2O, ppm) δ_H =2.33-2.35 (t, $2H_e$), 2.37-2.43 (m, $8H_{c,d}$), 2.73-2.77 (t, $2H_b$),

3.02-3.05 (t, $2H_a$) . ^{13}C NMR (D_2O, ppm) δ_C =36.69 (C_a), 38.03.4 (C_e), 52.01-53.89 ($C_{c,d}$), 57.52 (C_b).

<Please insert scheme 1>

2.5.2. *Synthesis of the ligands (H_2L^1 and H_2L^2)*

A solution of the prepared amine (0.5 mmol) in absolute ethanol (10 ml) was added drop wise to a solution of either 2-Hydroxybenzaldehyde or 2-hydroxy-3-methoxybenzaldehyde (1 mmol) in absolute ethanol (20 ml). After refluxing the solution for 12 h the resultant yellow powder was filtered off, washed with diethyl ether and dried under vacuum (scheme 2).

H_2L^1: Yield: 0.19 g (75%). EI-MS (m/z): 492. IR (KBr, cm^{-1}): 3428 ν(OH), 1637 ν(C=N). ^1H NMR ($CDCl_3$, ppm) δ_H= 2.54–2.57 (broad, $20H_{j-l}$), 2.69–2.73 (m, $4H_i$), 3.72-3.76 (m, $4H_h$), 6.86-7.33 (m, $8H_{a-f}$), 8.36 (s, $2H_g$), 13.45 (s, 2H(OH)). ^{13}C NMR ($CDCl_3$, ppm) δ_c= 53.66($C_{j,k}$), 55.91 (C_h), 57.07 (C_l), 58.69 (C_i), 117.04 (C_b), 118.51 (C_d), 118.79 (C_f), 131.21 (C_c), 132.22 (C_e), 161.19 (C_a), 165.59 (C_g).

H_2L^2: Yield: 0.19 g (75%). EI-MS (m/z): 552. IR (KBr, cm^{-1}): 3446 ν(OH), 1635 ν(C=N). ^1H NMR ($CDCl_3$, ppm) δ_H= 2.54–2.65 (broad, $20H_{j-l}$), 2.69–2.72 (t, $4H_i$), 3.72-3.76 (t, $4H_h$), 3.91 (s, $6H_{methoxy}$), 6.78-6.93 (m, $6H_{a-f}$), 8.33 (s, $2H_g$), 13.89 (s, 2H(OH)). ^{13}C NMR ($CDCl_3$, ppm) δ_c= 53.29-53.62 (C_{j-k}), 55.82 (C_h), 56.03 (C_{OCH3}), 56.55 (C_l), 58.57 (C_i), 113.71 (C_c), 117.69 (C_d), 118.41 (C_f), 122.81 (C_e), 148.55 (C_b), 152.3 (C_a), 165.56 (C_g).

<Please insert scheme 2>

2.5.3. *Synthesis of the metal complexes– general procedure*

To an ethanol solution of (H_2L^1 or H_2L^2) (0.5 mmol) was added either manganese perchlorate, zinc perchlorate or cadmium perchlorate (0.5 mmol) dissolved in absolute methanol and the solution was refluxed for 12 h. The resulting powder was filtered off and dried under vacuum.

2.5.3.1. [Mn(H_2L^1)(ClO_4)](ClO_4)

Brown powder. Yield: 0.21 g (77%). Anal. Calc. for $C_{28}H_{40}Cl_2MnN_6O_{10}$ (MW: 746.5): C, 45.05; H, 5.40; N, 11.26. Found: C, 44.49; H, 5.20; N, 11.06%. EI-MS (m/z): 648. IR (KBr, cm^{-1}): 3434 ν(OH), 1615 ν(C=N), 1197, 623 ν (ClO_4^-), 428 ν(M-N). Λ_m (CH_3CN)=176 $\Omega^{-1}cm^2$ mol^{-1}.

2.5.3.2. [Zn(H_2L^1)(ClO_4)](ClO_4)

Yellow powder. Yield: 0.21 g (74%). Anal. Calc. for $C_{28}H_{40}Cl_2ZnN_6O_{10}$ (MW: 756.03): C, 44.43; H, 5.33; N, 11.10. Found: C, 43.72; H, 5.53; N, 10.73%. EI-MS (m/z): 557. IR (KBr, cm^{-1}): 3443 ν(OH), 1623 ν(C=N), 1191, 624 ν (ClO_4^-), 468 ν(M-N). Λ_m (CH_3CN)=169 $\Omega^{-1}cm^2$ mol^{-1}. ^{1}H NMR (DMSO-d_6, ppm) δ_H=2.37-2.57 (m, $20H_{j-o}$), 2.65-2.73(m, $4H_h$), 3.72-3.83 (t, $4H_i$), 6.42-7 (m, $H_{b-e,\ t-w}$), 8.45 (s, H_g), 8.58 (s, H_r), 13.88 (s, $2H_{(OH)}$). ^{13}C NMR (DMSO-d_6, ppm) δ_c=29.3-31.5 ($C_{h,q}$), 51.7-52.1 ($C_{l,m}$), 52.5-54.4 ($C_{n,o}$), 54.7-55.7 ($C_{j,k}$), 57.9 (C_i), 59.4 (C_p), 110-163.7 ($C_{a-f,\ s-x}$), 166.3 (C_g), 168.8 (C_r).

2.5.3.3 [Cd(H_2L^1)(ClO_4)](ClO_4)

Yellow powder. Yield: 0.23 g (66%). Anal. Calc. for $C_{28}H_{40}Cl_2CdN_6O_{10}$ (MW: 804): C, 41.83; H, 5.02; N, 10.45. Found: C, 41.07; H, 5.36; N, 9.93%. EI-MS (m/z): 603. IR (KBr, cm^{-1}): 3431 ν(OH), 1633 ν(C=N), 1108, 625 ν (ClO_4^-), 402 ν(M-N). Λ_m (CH_3CN)=168 $\Omega^{-1}cm^2$ mol^{-1}. ^{1}H NMR (DMSO-d_6, ppm) δ_H=2.32-2.51 (m, $20H_{j-o}$), 2.51-2.58(t, $4H_h$), 3.65-3.75 (t, $4H_i$), 6.42-6.99 (m, $H_{b-e,\ t-w}$), 8.38 (s, H_g), 8.51 (s, H_r), 13.81 (s, $2H_{(OH)}$). ^{13}C NMR (DMSO-d_6, ppm) δ_c=29.3-

31.5 ($C_{h,q}$), 50-51.7 ($C_{l,m}$), 52-54.2 ($C_{n,o}$), 54.5-55.8 ($C_{j,k}$), 57 (C_i), 57.7 (C_p), 112.20-153.43 ($C_{a\text{-}f,\ s\text{-}x}$), 166.32 ($C_g$), 171.56 ($C_r$).

2.5.3.4. [Mn(H_2L^2)(ClO_4)](ClO_4)

Brown powder. Yield: 0.22 g (73%). Anal. Calc. for $C_{30}H_{44}Cl_2MnN_6O_{12}$ (MW: 806): C, 44.68; H, 5.50; N, 10.42. Found: C, 44.51; H, 5.22; N, 10.21%. EI-MS (m/z): 704. IR (KBr, cm^{-1}): 3456 ν(OH), 1614 ν(C=N), 1083, 624 ν (ClO_4^-), 462 ν(M-N). Λ_m (CH_3CN)=172 $\Omega^{-1}cm^2$ mol^{-1}.

2.5.3.5. [Zn(H_2L^2)(ClO_4)](ClO_4)

Yellow powder. Yield: 0.18 g (60%). Anal. Calc. for $C_{30}H_{44}Cl_2ZnN_6O_{12}$ (MW: 816.99): C, 44.10; H, 5.43; N, 10.29. Found: C, 44.51; H, 5.23; N, 9.87%. EI-MS (m/z): 620. IR (KBr, cm^{-1}): 3447 ν(OH), 1630 ν(C=N), 1108, 625 ν (ClO_4^-), 431 ν(M-N). Λ_m (CH_3CN)=193 $\Omega^{-1}cm^2$ mol^{-1}. ^{1}H NMR (DMSO-*d_6*, ppm) δ_H=2.15-2.73 (m, 20$H_{j\text{-}o}$), 2.73-2.84 (m, 4$H_{i,p}$), 3.63-3.73(m, 2H_q), 3.74-3.82 (s, 6$H_{(OCH3)}$), 3.84-3.9 (m, 2H_h), 6.45-7.13 (m, 6$H_{c\text{-}e,\ t\text{-}v}$), 8.47 (s, H_g), 8.61 (s, H_r), 13.91 (s, 2$H_{(OH)}$). ^{13}C NMR (DMSO-*d_6*, ppm) δ_c=53.1-53-3 ($C_{l,m}$), 56.1-56.3($C_{j,k}$), 56.6($C_{(OCH3)}$), 54.9-55.7 ($C_{n,o}$), 56.6 (C_i), 57.8 (C_h), 58.5 (C_p), 59.9 (C_q), 114.9-153.6 ($C_{a\text{-}f,\ s\text{-}x}$), 166.8 ($C_g$), 168.7 ($C_r$).

2.5.3.6. [Cd(H_2L^2)(ClO_4)](ClO_4)

Yellow powder. Yield: 0.23 g (69%). Anal. Calc. for $C_{30}H_{44}Cl_2CdN_6O_{12}$ (MW: 864): C, 41.7; H, 5.13; N, 9.73. Found: C, 41.03; H, 5.21; N, 9.24%. EI-MS (m/z): 764. IR (KBr, cm^{-1}): 3462 ν(OH), 1630 ν(C=N), 1189, 625 ν (ClO_4^-), 440 ν(M-N). Λ_m (CH_3CN)=182 $\Omega^{-1}cm^2$ mol^{-1}. ^{1}H NMR (DMSO-*d_6*, ppm) δ_H=2.03-2.65 (m, 20$H_{j\text{-}o}$), 2.65-2.83 (m, 4$H_{i,p}$), 3.59-3.64(m, 2H_q), 3.65-3.75 (s, 6$H_{(OCH3)}$), 3.76-3.8 (m, 2H_h) 6.26-6.99 (m, 6$H_{c\text{-}e,\ t\text{-}v}$), 8.27 (s, H_g), 8.50 (s, H_r), 13.82 (s, 2$H_{(OH)}$). ^{13}C NMR (DMSO-*d_6*, ppm) δ_c=51.52 ($C_{l,m}$), 51.8-53.2($C_{j,k}$), 54.4 ($C_{(OCH3)}$), 55.6-54.8 ($C_{n,o}$), 55.7 (C_i), 57.9 (C_h), 69.2 (C_p), 60.0 (C_q), 110-153.6 ($C_{a\text{-}f,\ s\text{-}x}$), 163.6 ($C_g$), 166.3 ($C_r$).

2.6. Cytotoxic assays

MTT assays were carried out to examine the cytotoxicity of the prepared complexes toward normal cells, and to investigate whether these complexes are able to exert antiproliferative effects against two cancer cell lines (A2780 and PC3) and a normal cell line (Fibroblast); these cell lines were supplied from Pasteur Institute of Iran. Cells were seeded and grown in DMEM medium (15-20×10^3 cells in each well) containing fetal bovine serum (10% v/v) and 1% penicillin/streptomycin (100 U/mL:100 U/mL). Culture plates were placed in a humidified incubator containing 5% CO_2 at 37 $^{\circ}$C. These cells were then exposed to different concentrations of the complexes in DMSO (12.5-100 µg/ml) and the samples incubated for 24 h. At appropriate time intervals, the medium was replenished with 0.5 mg/mL and then cells were incubated for further 3 h at 37 $^{\circ}$C. Thereafter, to enable the solubilizing of the formazan crystals, 100 µl DMSO was added to the culture medium. The controls and treated cells were subjected to an Eliza micro plate reader (Bio Tek Instruments, USA) to measure their absorbance at 570 nm. Cell viability percentage of each sample was calculated by dividing the absorbance at 570 nm, corresponding to each treatment group, to that of control group. The IC_{50} value (the concentration in which 50% of cells were killed) was calculated by preparing a logarithmic plot the viability percentage of cells versus the concentration of samples. All the MTT assays were carried out in triplicate.

2.7. Antibacterial assays

The antimicrobial activity of all synthesized compounds was assessed against four Gram positive and negative bacteria, namely *Staphylococcus aureus* (Wild), *Bacillus cereus* (PTCC 1247), *Pseadomonasaeroginesa* (PTCC 15442) and *Escherichia coli* (Wild) by the disc diffusion method [24]. All compounds were dissolved in DMSO to final concentrations of 50 and 100 mg/L. All tests were carried out using 10 mL of suspension cultures containing 1.5×10^{8} bacteria mL^{-1}, spread on nutrient agar medium. Negative controls were applied by using DMSO solution. Nitrofurantion and Neomycin and were used as positive standard references. A statistical analysis of the variance was performed using the Student's t-test, using the SPSS program, where a P value ≤ 0.05 was regarded as significant.

3. Result and discussion

A new polyamine (A) containing two piperazine moieties was synthesized and, using this amine, two new symmetrical, potentially N_6O_2 coordinating macroacyclic Schiff base ligands (H_2L^1 and H_2L^2) were prepared from the reaction with 2-Hydroxybenzaldehyde and 2-hydroxy-3-methoxybenzaldehyde, respectively. Six new macroacyclic Schiff base complexes were prepared from direct reaction of the two new Schiff base ligands (H_2L^1 and H_2L^2) with Mn(II), Zn(II) and Cd(II) metal ions. Elemental analysis confirm the synthesis of all compounds. The mass spectra show peaks at 648, 557, 603, 704, 620 and 764 for complexes $[Mn(H_2L^1)ClO_4]^+$, $[Zn(H_2L^1)]^{2+}$, $[Cd(H_2L^1)]^{2+}$, $[Mn(H_2L^2)ClO_4]^+$, $[Zn(H_2L^2)]^{2+}$ and $[Cd(H_2L^2)ClO_4]^+$ respectively.

3.1. IR spectra

IR spectrum of polyamine (A) exhibits a ν(NH_2) vibration in 3293-3443 cm^{-1}. IR spectra of both ligands exhibit a ν(C=N) vibration in 1637 cm^{-1} and 1635 cm^{-1} and do not show any bands expected for the free carbonyls or primary amines, indicating that complete condensation has occurred. In the IR spectra of the metal complexes, the ν(C=N) band is shifted to lower frequency (1614–1633 cm^{-1}), compared to that found the free ligands, confirming the coordination of the metal to the ligand. Absorption bands at approximately 1100 and 620 cm^{-1} arising from the perchlorate anions were found to be split, indicating that the perchlorate anions were coordinated to metal ions. A broad band at approximately 3400 $cm^{-1}$is due to the OH group of the ligand, indicating that that deprotonation does not occur in the metal complexes. Furthermore, new weak bands in the range of 402-468 cm^{-1} are attributed to the M-N bonds.

3.2. NMR spectra

The ^{13}C NMR spectrum of polyamine (A) shows four main peaks (36.6-57.5 ppm), while in the ^{1}H NMR spectrum a broad signal for the amine protons appears at 2.4 ppm due to proton exchange in D_2O solvent. In the ^{1}H NMR spectra of H_2L^1 and H_2L^2 the signal for the imine proton appears at 8.3 ppm, while the signal for the hydroxyl protons appear at 13.4 and 13.8 ppm respectively. There were no signals due to amine protons, confirming the complete synthesis of the Schiff base ligands. In ^{13}C NMR spectrum of H_2L^1 and H_2L^2, the number of peaks and their chemical shifts are also consistent with the ligand structures. Using the DEPT 135 technique the spectrum of H_2L^1 shows 10 peaks including 5 positive and 5 negative peaks which are related to CH groups and CH_2 groups respectively, while 2 peaks (161.1 and 118.7 ppm) related to C_a and C_f are no longer present. The spectrum of H_2L^2 shows 10 peaks including 5 positive and 5 negative peaks which are related to CH, CH_3 (56 ppm) groups and CH_2 groups respectively,

while 3 peaks (152.3, 148.5and 118.4 ppm) related to C_a, C_b and C_f are no longer present. The ^{1}H NMR spectra of the complexes showed two peaks indicating two non-equivalence imine groups in the zinc and cadmium complexes: 8.4 and 8.5 ppm $[Zn(H_2L^1)]^{2+}$, 8.4 and 8.6 ppm $[Zn(H_2L^2)]^{2+}$, 8.3 and 8.5 ppm $[Cd(H_2L^1)]^{2+}$ and 8.2 and 8.5 ppm $[Cd(H_2L^2)]^{2+}$, shifted respect to the corresponding signal in the free ligand. The signal of the hydroxyl protons appears at 13.8-14.00 ppm, indicating that two phenolic OH groups are not deprotonated. Slight frequency shifts are also observed for the aromatic protons when compared with the free ligands. The ^{13}C NMR spectra of the complexes show two peaks corresponding to the imine carbon atoms showing that two imine carbon atoms are not identical. These peaks were appeared at 168.8 and 166.3 ppm in $[Zn(H_2L^1)]^{2+}$, 168.7 and 166.8 ppm in $[Zn(H_2L^2)]^{2+}$, 171.5 and 166.3 ppm in $[Cd(H_2L^1)]^{2+}$, 166.3 and 163.6 ppm in $[Cd(H_2L^2)]^{2+}$ The symmetry of metal complexes is reduced, so the number of peaks appearing in the ^{13}C NMR spectra of the metal complexes were more than was found for the free ligands. There should be 28 and 29 main peaks in the ^{13}C NMR spectra of the ($[Zn(H_2L^1)]^{2+}$, $[Cd(H_2L^1)]^{2+}$) complexes and ($[Zn(H_2L^2)]^{2+}$, $[Cd(H_2L^2)]^{2+}$) complexes, respectively, however overlapping of peaks would be expected due to the similarity of several of the carbon atoms, and the low resolution of instrument.

3.3. Molar conductivity

The molar conductance values can be predicted by the electrolytic nature of the mononuclear metal complexes. Herein, the molar conductivity values for all mononuclear complexes in MeCN are in or slightly above the literature range for a 1:1 electrolyte in MeCN (120-160 $cm^2\ \Omega^{-1}\ mol^{-1}$, but values as high as 199 $cm^2\ \Omega^{-1}\ mol^{-1}$ have been used to characterize 1:1 electrolytes in

MeCN) [25]. All of these values are consistent with existence the perchlorate group as counter anion in the complexes.

3.4. X-ray structure

Light yellow single crystals of H_2L^1 were crystallized by slow evaporation from methanol. Crystallographic data and structure refinement parameters are given in Table 1 and selected bond lengths and angles are given in Table 2.

The molecule is situated around a center of symmetry and adopts an extended, almost linear arrangement (Figure 1). The phenol hydrogen is involved in an intramolecular hydrogen bond with the imine nitrogen. The atoms of the imine group are coplanar with the phenol group, the maximum deviation from the plane being 0.0475(9) Å. The piperazine ring is in a chair conformation, the dihedral angle between the four carbon atoms of the ring and the phenol ring being 14.77(7)°. There are no significant intermolecular contacts.

<Please insert Fig. 1>

<Please insert Table 2>

3.5. Stoichiometry and stability constant

The ^7Li chemical shifts were monitored as a function of the mole ratio of metal to the macroacyclic Schiff base ligands H_2L^1 and H_2L^2 in both acetonitrile and methanol. In all cases, the presence of only a single ^7Li resonance reveals that the exchange rate of Li^+ ion between the

bulk solution and the complexed sites is fast on the NMR time scale (Fig. 2). *All the resulting ^{7}Li chemical shifts as a function of the $[H_2L^1]/[M^{n+}]$ mole ratio are illustrated in Figure 3*. As can be seen, in the absence of other metal ions (Li^+ curves with H_2L^1 in Fig. 2A), addition of H_2L^1 or H_2L^2 Schiff base ligand to the lithium ion solution causes an almost linear paramagnetic shift in the observed ^{7}Li chemical shift, δ_{obs}, which is due to the population-averaged combination of the chemical shifts of Li^+ ion in the bulk solvent, δ_{Li}, with that of the Li^+ ion complexed with ligand, δ_{LiH2L}, values that are quite different due to differences in the electron densities surrounding the probe nucleus in the two sites, $\delta_{obs} = P_{Li}\,\delta_{Li} + P_{LiH2L}\,\delta_{LiH2L}$ (where, $P_{Li} + P_{LiH2L} = 1$ in the course of titration of metal ion with the ligand). The variations of ^{7}Li chemical shift with the H_2L/Li^+ mole ratio were used to calculate the formation constants of Li^+←complexes with Schiff base ligands.

Assuming that the fast-exchange kinetics prevail, it has been shown that in solutions containing fixed concentration of Li^+ by varying amount of ligand, C_{H2L}, the observed chemical shift of the metal ion is given by [26]:

$$\delta_{obs} = \Big\{ [(K_{Li}C_{\mathrm{Li}} - K_{\mathrm{Li}}C_{H_2L} - 1) + (K_{\mathrm{Li}}^2C_{H_2L}^2 + K_{\mathrm{Li}}^2C_{\mathrm{Li}}^2 - 2K_{\mathrm{Li}}^2C_{H_2L}C_{\mathrm{Li}} + 2K_{\mathrm{Li}}C_{H_2L} + 2K_{\mathrm{Li}}C_{\mathrm{Li}} + 1)^{1/2}](\delta_{\mathrm{H_2L}} - \delta_{\mathrm{Li}-H_2L})/2K_{\mathrm{Li}}C_{\mathrm{Li}} \Big\} + \delta_{\mathrm{Li}-H_2L} \qquad \text{Eq. 1}$$

Where δ_{Li} and $\delta_{Li\text{-}H2L}$ are the respective chemical shifts of the free and complexed Li^+ ion. The nonlinear least-squares curve fitting program KINFIT [27] was used to evaluate K_{Li} and $\delta_{Li\text{-}H2L}$ values. In this paper, we were interested in investigating the complexation of Cd^{2+}, Zn^{2+} and Mn^{2+} ions with H_2L^1 and H_2L^2 in methanol and acetonitrile solutions. These cations have unsuitable NMR properties, such as high quadrupole moment, low receptivity, insensitive

chemical shifts, etc. [28]. Therefore, in this paper, we employed ^{7}Li NMR as a more sensitive probe [29-32] to study the formation of the resulting complexes of Mn^{2+}, Zn^{2+} and Cd^{2+} ions with H_2L^1 and H_2L^2 in solutions. Solutions containing Li^+ and each of the M^{2+} ions with the concentration of both metals being 0.01 M, were titrated with each of the Schiff base ligands (H_2L^1 and H_2L^2), while monitoring the chemical shift changes of the ^{7}Li nucleus in solution [33-36]. The plots of the ^{7}Li chemical shift in the presence of equimolar concentrations of M^{2+} ions and Li^+ (0.01 M) as a function of H_2L/M^{n+} mole ratio in acetonitrile and methanol solutions are shown in figure 3. As it is obvious from Figures 2 and 3, the change in chemical shift with the H_2L/M^{n+} mole ratio is quite linear at mole ratio less than 1, the mole ratio plots in the presence of other used M^{2+} ions show a small change in chemical shift of the Li^+ ion at H_2L/ M^{n+} mole ratios between 0 and 1, followed by a sharp linear increase in $\delta_{obs,}$ which begins to level off at mole ratios bigger than 2. The resulting mole ratio plots show that, due to the higher stability of the M^{2+}-H_2L complexes over the Li^+-H_2L complex, most of the ligand complexes with the M^{2+} ion at H_2L/ M^{n+} mole ratios less than 1 so that most of the Li^+ ions remain free in solution and, thus, the ^{7}Li chemical shift changes only slightly. However, at mole ratios larger than 1, where the amount of free M^{2+} ions in solution very small, the Li^+ ions are able begin to form 1:1 complexes with the added ligand and, thus, the δ_{obs}-mole ratio behavior at mole ratios larger than 1 shows a trend similar to that observed in the case of titration of Li^+ ion alone with the ligand (see Figs. 2B and 3), indicating the quantitative formation of 1:1 complexes of the ligands with all three studied M^{2+} ions.

<Please insert Fig. 2>

<Please insert Fig. 3>

The competitive complexation equilibria for the case of 1:1 complexation between Schiff base ligands and Li^+ and the M^{2+} ions can be written as:

$$Li^+ + H_2L \Leftrightarrow Li^+H_2L \qquad K_{Li} = [Li^+H_2L]/[Li^+][H_2L] \qquad \text{Eq. 2}$$

$$M^{2+} + H_2L \Leftrightarrow M^{2+}H_2L \qquad K_M = [M^{2+}H_2L]/[M^{2+}][H_2L] \qquad \text{Eq. 3}$$

The free Schiff base ligand concentration is then obtained from Eq. 4 [37].

$$K_{Li}K_M[H_2L]^3 - \{K_{Li}K_M(C_{H_2L} - C_{Li} - C_M) - K_{Li} - K_M\}[H_2L]^2$$
$$-\{K_{Li}(C_{H_2L} - C_{Li}) + K_M(C_{H_2L} - C_M) - 1\}[H_2L - 1][H_2L] - C_{H_2L} = 0 \qquad \text{Eq. 4}$$

Where C_{H2L}, C_{Li}, and C_M are the analytical concentrations of the ligand, Li^+ and M^{2+} ion, respectively and K_{Li} calculated by Eq. 1. In this case, the observed [^{7}Li] NMR chemical shift is obtained from Eq. 5 [30].

$$\delta_{obs} = P_{Li}\delta_{Li} + P_{LiH_2L}\delta_{LiH_2L} \qquad \text{Eq. 5}$$

Where P_{Li} and P_{LiH2L} are the mole fractions of the free and complexed lithium ion, respectively. By substitution from Eq. 2 and the mass balance equation $C_{Li}=[Li^+] + [Li^+H_2L]$, Eq. 5 can be written as:

$$\delta_{obs} = \{\delta_{Li} + \delta_{LiL}[H_2L]K_{Li}\}/\{1 + K_{Li}[H_2L]\} \quad \text{Eq. 6}$$

The K_M values were evaluated by obtaining the free Schiff base ligand concentration from Eq. 4 and fitting the chemical shift-mole ratio data to Eq. 6 by using the KINFIT program [38]. A computer fit of the data is displayed in Figure 4 and the resulting log K_f values are collected in Table 3. Our assumption that the 1:1 stoichiometry for both M^{2+}-H_2L complexes seems reasonable in the light of a reasonable agreement between the observed and calculated chemical shifts.

<Please insert Fig. 4>

<Please insert Table 3>

The observed stability constants of the in situ generated complexes are significantly affected by two main factors, the nature of counter anions and the concentrations of the salts used. Ion pair formation, between the metal ions and their counter anions, may also have an effect. Thus, in this work, we used the same salt concentration of 0.01 M with the same counter anions, to ensure the constant effect of concentration and counter anion on stability constants of all the complexes. The results in Table 3 confirmed that, in both solvents and all three studied metal ions, the

resulting complexes of two ligands vary in the order of MH_2L^1> MH_2L^2. This is due to the fact that two Schiff base ligands (H_2L^1 and H_2L^2) differ in the substituted groups (Scheme 2).

The information in Table 3 clearly indicate that, the stability of the resulted complexes changes in the order of Mn^{2+}<Zn^{2+}<Cd^{2+} in both solvents. The stability of the complexes are controlled by several factors comprising:(i) the scope of interaction between donor atoms (nitrogen and oxygen) of Schiff base ligands with the cations, (ii) the adaption between the size of metal ions and the steric size of the formed Schiff base ligands distortion, (iii) soft-hard acid-base concept of the metal ion and the donor atoms of the nitrogen and oxygen, (iv) desolvation of cation and the donors and solvation of the macroacycle. The factors (iii) and (iv) depend significantly on the nature of the solvents employed. On the NMR time scale, the stability of the Mn^{2+} and Zn^{2+} complexes with both Schiff base ligands was changed in the order of Zn^{2+}>Mn^{2+}, most probably because of its ionic solvation in the solvents used [39]. The results display the highest stability for Cd^{2+} complexes with both Schiff base ligands between all three employed M^{2+} ions. This is most likely due to the larger size of the Cd^{2+} ion at soft nature, which could coordinate better with the donor atoms of the relatively large and flexible Schiff base ligands [40-42]. Based on given data in Table 3, the stability of the formed complexes depended on the solvent combination. In all cases, the resulting complexes are more stable in acetonitrile than in methanol. It should be noted that, while acetonitrile and methanol have about the same dielectric constants (i.e., D=33.0 for methanol and D=36.1 for acetonitrile), their solvating abilities, as expressed by the Gutmann donor number [43], are different (i.e., DN =79.0 kj/mol for methanol and DN = 59.0 kj/mol for acetonitrile). *Thus, methanol, which has a higher solvating ability compared to acetonitrile, can compete more strongly with the Schiff base ligands for the metal*

ions than can acetonitrile. Consequently, formation of the weaker complexes is more likely to occur in methanol than in acetonitrile.

3.6. Cytotoxicity activities

In order to examine whether the prepared complexes can inhibit the proliferation of ovarian and prostate cancer cells, the viability of these cells before and after exposure of complexes were compared. As well, the toxicity of these newly synthesized complexes toward normal fibroblast cells were also examined to ensure the non-toxic nature of these products (Figure 5(a)). As can be seen the figure obviously indicated that all the six complexes were non-toxic for normal cells (viability percentage >60% even at the highest concentration) and none of the curves reached IC_{50} value, whereas these samples all significantly decreased the viability of A2780 ovarian cancer cells in a dose-dependent manner, they all were potent in killing more than 50% of cells. The IC_{50} value of four samples ($[Zn(H_2L^2)(ClO_4)](ClO_4)$, $[Cd(H_2L^2)(ClO_4)](ClO_4)$, $[Mn(H_2L^1)(ClO_4)](ClO_4)$, and $[Cd(H_2L^1)(ClO_4)](ClO_4)$ were the same (about 12.5 μg/ml), however the $[Mn(H_2L^1)(ClO_4)](ClO_4)$ complex possessed a less toxic effect toward A2780 (IC_{50} value of 25 μg/ml). The least toxic effect on ovarian cancer cells could be attributed to the complex $[Zn(H_2L^1)(ClO_4)](ClO_4)$, which killed 50% of cells at concentration about 100 μg/ml. The antiproliferative effect of these compounds would be necessarily compared with the metal-based cytotoxic compounds that are commonly used for the treatment of cancer, such as cisplatin. There are several studies reporting the toxicity of cisplatin toward different cancer cells. Cisplatin, as a standard anticancer drug, possessed significant effect against A2780 and PC3 cells. The IC50 concentration has been found to be almost 0.73-2.8 μM (0.219-0.842 μg/ml)

in previous studies [44, 45]. The comparison between the present compounds and cisplatin reveals that although these compounds have less potent anticancer activity, in comparison to cisplatin, their toxic concentrations are in an acceptable range. These results confirmed that the synthesized complexes in the present study could be promising candidates for preparing novel chemotherapeutics against ovarian carcinoma, especially as the results also show that these compounds exert no toxicity toward normal fibroblast cells. The other similar study on macrocyclic complexes containing piperazine have shown to be great agents against A2780 cells [20, 46]. Herein, the results also indicated that all the samples, were not able to affect PC3 prostate cancer cells significantly except $[Cd(H_2L^2)(ClO_4)](ClO_4)$ complex which was reached the IC_{50} value at the used concentration (100 μg/ml), while the IC50 value of cisplatin has been reported to be 2.3 μM(0.690 μg/ml) toward PC3 cells [45]. These results could be used as starting point for our research program to introduce the potent compounds as novel anticancer agents. Further studies on the effect of these compounds against other types of normal cells, and also in experimental animals, would be beneficial to provide a definite conclusion, and to unequivocally ensure the safety of these compounds as anticancer agents. Furthermore, investigations on the mechanism of action of these compounds against ovarian cancer cells would be of a great importance.

<Please insert Fig. 5>

3.7. Antibacterial activities

The antibacterial activity of all compounds were studied against four types of Gram positive and negative bacteria, compared with the antibacterial activity of two antibiotics. All compounds were dissolved in 2 different concentrations of DMSO. Also, DMSO (used as the solvent) was screened against all bacteria included in this work and no activity was found. The antibacterial activities of all compounds were increased with an increase in the concentration of the samples (Table 4). It was found that metal complexes have higher activities than the free ligands against all bacterial strains tested. Generally, the metal complexes $[Zn(H_2L^1)(ClO_4)](ClO_4)$, $[Cd(H_2L^1)(ClO_4)](ClO_4)$ and then $[Mn(H_2L^1)(ClO_4)](ClO_4)$ showed more antibacterial activity against all bacterial species than other samples, which were even greater than the standard antibiotics of neomycin and nitrofurantion. In contrast, the samples H_2L^1 and H_2L^2 represented the weakest activity against the bacterial tested, except for *B. cereus*. The other samples gave different activities against the studied bacteria.

<Please insert Table 4>

Description of the proposed structures of the complexes

Starting from a metal:ligand mole ratio of 1, where M=Zn (II), Mn (II), Cd (II), mononuclear complexes have been obtained. Unfortunately, our attempt to get suitable single crystals for X-ray structural analyses were unsuccessful. Accordingly, all the complexes were characterized by a number of physicochemical techniques. In the IR spectra of complexes, the shift of ν(C=N) to lower frequency, the splitting of the perchlorate bands, the existence the broad bands in the

range 3431-3462 cm^{-1} related to OH groups and the appearance of new weak bands in the range of 402-468 cm^{-1}, attributed to the M-N bonds, are important features of spectra. In the ^{1}H NMR spectra of the complexes, two signals related to the imine protons are shifted with respect to the corresponding signal in the free ligand, indicating that the two imino groups are non-equivalent. As well, the presence of hydroxyl proton signals in the ^{1}H NMR spectra confirms that the two phenolic OH moieties did not deprotonate upon complex formation. Furthermore, the ^{13}C NMR spectra of the complexes show two peaks corresponding to the imine carbon atoms, indicating that the symmetry of ligands was reduced in the complexes. An increase in the number of peaks in the ^{13}C NMR spectra of the complexes, compared to the free ligands, confirm the unsymmetrical structure of complexes. The molar conductivity data indicates that all complexes are electrolytes due to the presence of one counter ion in their structures. Stoichiometry and stability constant data clearly indicate that the 1:1 M^{2+}-H_2L complexes are formed in non-aqueous solvents. Based on this information we propose that $[M(H_2L)(ClO_4)](ClO_4)$ has a distorted pentagonal bipyramidal geometry with the azomethine nitrogen and the nitrogen atoms of piperazine rings coordinating to the metal in the equatorial plan, with the azomethine nitrogen and perchlorate anion coordinating in the axial positions. Mass spectra and elemental analysis are consistent with the proposed structure.

4. Conclusion

In summary, this paper describes the synthesis and spectroscopic characterization of a series of manganese (II), cadmium (II) and zinc (II) complexes with two new Schiff base ligands derived from piperazine. The molecular structure of ligand H_2L^1 has been determined by a single crystal X-ray structural analysis. The complexes have been characterized by a number of

physiochemical techniques. It is proposed that these complexes have a distorted pentagonal bipyramidal geometry with the metal coordinated by the six donor atoms of the ligand and one perchlorate. The Nuclear Magnetic Resonance stoichiometry study clearly indicates that the 1:1 M^{2+}-H_2L complexes are formed in non-aqueous solvents. All of the synthesized complexes have been investigated for antibacterial activities. The metal complexes $[Zn(H_2L^1)(ClO_4)](ClO_4)$ and $[Cd(H_2L^1)(ClO_4)](ClO_4)$ and then $[Mn(H_2L^1)(ClO_4)](ClO_4)$ showed more antibacterial activity against all bacterial species than other samples; their activity was even greater than the standard antibiotics of neomycin and nitrofurantion. We studied the cytotoxic activity of all complexes on ovarian and prostate cancer cells. All synthesized samples significantly decreased the viability of A2780 ovarian cancer cells however none of the samples, except for $[Cd(H_2L^2)(ClO_4)](ClO_4)$, were able to affect PC3 prostate cancer cells.

5. Supplementary data

CCDC 1861798 contains the supplementary crystallographic data for $[H_2L^1]$ compound. This data can be obtained free of charge via http://www.ccdc.cam.ac.uk/conts/retrieving.html, or from the Cambridge Crystallographic Data Centre, 12 Union Road, Cambridge CB2 1EZ, UK; fax: (+44) 1223-336-033; or e-mail: deposit@ccdc.cam.ac.uk.

Acknowledgements

We are grateful to the Faculty of Chemistry of Bu Ali Sina University, for financial supports.

References:

[1] M. Rezaeivala, H. Keypour, Coord. Chem. Rev. 280 (2014) 203.

[2] A.D. Granvoskii, A.L. Nivorozhkin, V.I. Minkin, Coord. Chem. Rev. 126 (1993) 1.

[3] M.A.V. Ribeiro Da Silva, M.D.M.C. Ribeiro Da Silva, M.J.S. Monte, J.M. Goncalves, E.M.R. Fernandes, J. Chem. Soc., Dalton Trans. (1997) 1257.

[4] H. Keypour, N. Rahpeyma, P. Arzhangi, M. Rezaeivala, Y. Elerman, O. Buyukgungor, L. Valencia, Polyhedron. 29 (2010) 1144.

[5] H. Keypour, N. Rahpeyma a, M. Rezaeivala, P. Arzhangi, M. Bayat, L. Valencia, Y. Elerman, O. Buyukgungor, Polyhedron. 51 (2013) 117.

[6] H. Keypour, M. Rezaeivala, M. Mirzaei-Monsef, K. Sayin, N. Dilek, H. Unver, Inorg. Chim. Acta. 432 (2015) 243.

[7] H. Keypour, A. Shooshtari, M. Rezaeivala, M. Bayat, H. AmiriRudbari, Inorg. Chim. Acta. 440 (2016) 139.

[8] H. Keypour, M. Rezaeivala, A. Ramezani-Aktij, M. Bayat, N. Dilek, H. Ünver, J. Mol. Struct. 1115 (2016) 180.

[9] R. Malcolm, H. Trafford, UK patent. 2 222 768, 1990; C.A., 113, 204833k (1990).

[10] A. M. Oficialdegui, J. Martinez, S. Perez, B. Heros, M. Iruzuny, J. A. Palop, R. Tordera, B. Lasheros, J. RioDel, A. Mange, Farmaco. 55(4), 345 (2000); C. A., 133, 305272v (2000).

[11] A. Chan Mug, T. Jung Ae, Ch. Sun Ju, Arch. PharmacolRes. 23(4), 288 (2000); C. A., 133, 335196r (2000).

[12] H. Keypour, M. Rezaeivala, L. Valencia, P. Pérez-Lourido, Polyhedron. 27 (2008) 3172.

[13] R. V. Patel, S. W. Park, Mini-Rev. Med. Chem. 13 (2013) 1579.

[14] H. Keypour, M. Rezaeivala, L. Valencia, P. Pérez-Lourido, A. H. Mahmoudkhani, Polyhedron. 28 (2009) 3415.

[15] H. Keypour, M. Rezaeivala, L. Valencia, S. Salehzadeh, P. Pérez-Lourido, H. R. Khavasi, Polyhedron. 28 (2009) 3533.

[16] H. Keypour, M. Rezaeivala, L. Valencia, P. Pérez-Lourido, Polyhedron. 28 (2009) 4096.

[17] H. Keypour, M. Rezaeivala, L. Valencia, P. Pérez-Lourido, H. R. Khavasi, Polyhedron. 28 (2009) 3755.

[18] H. Keypour, M. Mahmoudabadi, A. Shooshtari, M. Bayat, R. Karamian, M. Asadbegy, R. W. Gable, Inorg. Chim. Acta. 478 (2018) 176.

[19] H. Keypour, M. Mahmoudabadi, A. Shooshtari, M. Bayat, F. Mohsenzadeh, R. W. Gable, J. Mol. Struct. 1155 (2018) 196.

[20] H. Keypour, M. Mahmoudabadi, A. Shooshtari, L. Hosseinzadeh, F. Mohsenzadeh, R. W. Gable, Polyhedron. 127 (2017) 345.

[21] O. V. Dolomanov, L. J. Bourhis, R. J. Gildea, J. A. K. Howard, H. Puschmann, J. Appl. Cryst. 42 (2009) 339.

[22] G. M. Sheldrick, ActaCryst. A71 (2015) 3-8.

[23] G. M. Sheldrick, ActaCryst. C71 (2015) 3-8.

[24] A.W. Bauer, M.M. Kirby, J.C. Sherris, M. Truck, Am. J. Clin. Pathol. 45 (1966) 493.

[25] W, Geary, Coord. Chem. Rev. 7 (1971) 81.

[26] E.T. Roach, P.R. Handy, A.I. Popov, Inorg. Nucl. Lett. 9 (1973) 359.

[27] V.A. Nicely, J.L. Dye, J. Chem. Educ. 48 (1971) 443.

[28] R.K. Harris, B.E. Mann, NMR and the Periodic Table. Academic Press, New York, (1978).

[29] J. Kim, M. Shamsipur, S.Z. Huang, R.H. Huang, J. L. Dye, J. Phys. Chem. A 103 (1999) 5615.

[30] M. Shamsipur, A.I. Popov, J. Am. Chem. Soc. 101(1979) 4051.

[31] B.O. Strasser, M. Shamsipur, A.I. Popov, J. Phys. Chem. 89 (1985) 4822.

[32] M. Shamsipur, A.I. Popov, J. Phys. Chem. 91(1987) 447.

[33] H. Keypour, M.H. Zebarjadian, S.J. Sabounchei, J. Iranian Chem. Soc. 14 (2014) 464.

[34] H. Keypour, M.H. Zebarjadian, M. Rezaeivala, M. Shamsipur, H.R. Bijanzadeh, J. Solution Chem. 14 (2014) 196.

[35] H. Keypour, M.H. Zebarjadian, M. Rezaeivala, A. Afkhami, J. Mol. Struct. 20 (2014) 796.

[36] E. Karkhaneei, M.H. Zebarjadian, M. Shamsipur, J. Solution Chem. 30 (2001) 4.

[37] Ghasemi, J., Shamsipur, M, J. Coord. Chem. 31 (1994) 265.

[38] Shamsipur, M., Karkhaneei, E., Afkhami, A, J. Coord. Chem. 44 (1998) 23.

[39] A. Semnani, M. Shamsipur, J. Electroanal Chem. 315 (1991) 95.

[40] J. Burger, Ionic Solvation and Complex Stability Reactions in Non-aqueous Solvents, AkdemiaiKiado, Budapest, 1993.

[41] M. Shamsipur, N. Alizadeh, Talanta. 39 (1992) 1209.

[42] T. Madrakian, M. Shamsipur, Polish J. Chem. 73 (1999) 1405.

[43] V. Gutmann, The Donor-Acceptor Approach to Molecular Interactions, Plenum Press, New York (1978).

[44] Allison, S.J., Sadiq, M., Baronou, E., Cooper, P.A., Dunnill, C., Georgopoulos, N.T., Latif, A., Shepherd, S., Shnyder, S.D., Stratford, I.J., Wheelhouse, R.T, *Cancer letters*, (2017) 98.

[45] Raveendran, R., Braude, J.P., Wexselblatt, E., Novohradsky, V., Stuchlikova, O., Brabec, V., Gandin, V., Gibson, D., *Chemical Science* (2016) 2381.

[46] Keypour, H., Mahmoudabadi, M., Shooshtari, A., Bayat, M., Ghassemzadeh, M., Hosseinzadeh, L., Mohsenzadeh, F., Harms, K., *Polyhedron* (2017) 189.

Table 1.

Crystal data and structure refinement for H_2L^1.

Crystal data	
Identification code	rwg2018_18Gau
Empirical formula	$C_{28}H_{40}N_6O_2$
Formula weight	492.66
Temperature/K	130.00(10)
Crystal system	monoclinic
Space group	I2/a
a/Å	9.4074(3)
b/Å	5.7404(2)
c/Å	49.0645(14)
α/°	90
β/°	90.442(3)
γ/°	90
Volume/Å^3	2649.51(16)
Z	4
ρ_{calc}g/cm^3	1.235
μ/mm^{-1}	0.632
F(000)	1064.0
Crystal size/mm^3	0.448 × 0.125 × 0.12
Radiation	CuKα (λ = 1.54184)
2Θ range for data collection/°	7.206 to 154.384
Index ranges	$-11 \leq h \leq 11$, $-7 \leq k \leq 7$, $-61 \leq l \leq 52$
Reflections collected	12671
Independent reflections	2788 [R_{int} = 0.0263, R_{sigma} = 0.0167]
Data/restraints/parameters	2788/0/244
Goodness-of-fit on F^2	1.059
Final R indexes [I>=2σ (I)]	R_1 = 0.0363, wR_2 = 0.0964
Final R indexes [all data]	R_1 = 0.0387, wR_2 = 0.0990
Largest diff. peak/hole / e Å^{-3}	0.22/-0.16

Table 2.
Bond lengths and bond angles for H_2L^1.

H_2L^1			
Bond	**Angle(°)**	**Bond**	**Length(Å)**
C7-N1-C8	119.48(9)	O1-C1	1.3494(13)
C9-N2-C10	109.15(7)	N1-C7	1.2757(14)
C9-N2-C13	111.24(8)	N1-C8	1.4593(13)
C10-N2-C13	108.76(7)	N2-C9	1.4622(12)
C11-N3-C12	108.50(7)	N2-C10	1.4629(12)
C11-N3-C14	111.11(8)	N2-C13	1.4668(12)
C12-N3-C14	109.77(7)	N3-C11	1.4635(12)
O1-C1-C2	119.02(10)	N3-C12	1.4647(12)
O1-C1-C6	121.44(9)	N3-C14	1.4661(12)
C2-C1-C6	119.54(10)	C1-C2	1.3960(15)
C3-C2-C1	120.24(11)	C1-C6	1.4098(15)
C2-C3-C4	120.94(11)	C2-C3	1.3799(17)
C5-C4-C3	119.18(11)	C3-C4	1.3881(19)
C4-C5-C6	121.24(11)	C4-C5	1.3847(16)
C1-C6-C7	120.97(9)	C5-C6	1.3978(14)
C5-C6-C1	118.85(10)	C6-C7	1.4619(14)
C5-C6-C7	120.17(10)	C8-C9	1.5181(14)
N1-C7-C6	120.81(10)	C10-C11	1.5132(12)
N1-C8-C9	107.66(8)	C12-C13	1.5160(13)
N2-C9-C8	113.45(8)	C14-C14[1]	1.5201(18)
N2-C10-C11	111.23(8)		
N3-C11-C10	111.15(8)		
N3-C12-C13	111.46(8)		
N2-C13-C12	111.02(8)		
N3-C14-C14[1]	112.28(10)		

Table 3.

Formation constants for metal ion complexes with H_2L^1 and H_2L^2 in methanol and acetonitrile solutions at 25°C.

	Logk_f			
	Methanol		**Acetonitrile**	
Cation[a]	**H_2L^1**	**H_2L^2**	**H_2L^1**	**H_2L^2**
Cd^{2+}(0.83)	2.80±0.04	2.59±0.03	4.17±0.06	3.81±0.05
Zn^{2+}(0.74)	2.42±0.06	2.27±0.02	3.83±0.04	3.58±0.03
Mn^{2+}(0.95)	1.58±0.05	1.41±0.04	2.98±0.02	2.79±0.04

Values in parentheses are the ionic radius of cations in

Table. 4.

Antibacterial activity of complexes that was expressed as diameter of inhabitation zone (mm).

	Zone of inhabitation (mm)									
Microorganisms	**Standard**		**Synthesized compounds**							
	Neomycin$^{\beta}$	**Nitrofurantion$^{\beta}$**	**H_2L^1**	**ZnL^1**	**MnL^1**	**CdL^1**	**H_2L^2**	**ZnL^2**	**MnL^2**	**CdL^2**
E.coli	21.33±0.57	24±1	7.5^{b} ±0.5* 10.16^{b} ±0.76**	14.16^{b}±0.76* 17.16^{b} ±1.8**	11^{b}±1* 16.5^{b}±0.5**	11.16^{b}±1.04* 16.16^{b}±1.04**	8.1^{b}±1.04* 8.5^{c}±1.5**	9.33^{b}±1.04* 13.66^{b}±1.25**	8.1^{b}±1.25* 14.84^{b}±0.76**	13.33^{b}±1.5* 13.33^{a} ±1.52**
P. aeroginesa	21.33±0.57	25.33±1.15	10.0^{a}±1 * 12.16^{a}±1.04**	23.33^{a} ± 1.52* 26^{a} ± 1**	14.36^{a}±1.26* 18.16^{a}±0.76**	18.3^{a}±1.52* 19.66^{a}±1.52**	10.33^{a}±152* 10.66^{a}±1.55**	18.5^{a}±0.86* 19^{a}±1.7**	15.5^{a}±0.5* 17.0^{a}±1**	15.8^{a}±0.76* 16.33^{a}±1.52**
S. aureus	NA	NA	NA	14.33^{b} ±.5* 19^{c} ±.1**	8.0^{c}±0.5 * 14.0^{c}±1**	13.0^{b}±1* 14.66^{b}±1.04**	NA* 8.16^{c}±0.76**	7.5^{b}±0.5* 15.16^{b}±1.7**	7.5^{b}±0.5* 13.33^{b}±1.52**	8.0^{c}±0.5* 8.0^{b}±1**
B. cereus	19.16±0.76	25.66±0.22	NA* 8.3^{c}±1.04**	8^{c} ±1* 13.5^{b} ± 1.5**	NA* 8.83^{d}±1.6**	7.5^{c}±0.5* 8.83^{c}±1.04**	7.8^{b}±0.57* 9.5^{ab}±0.5**	NA* 8.33^{c}±0.76**	NA	8.0^{c}±1* 9.0^{b}±1**

Experiment was performed in triplicate and expressed as mean ± SD.
*sample concentration=50 mg/L & **sample concentration=100 mg/L
$^{\beta}$Positive controls
NA=No active

Scheme 1. The processes of synthesis of 2,2'-(ethane-1,2-diylbis(piperazine-4,1-diyl))bis(ethan-1-amine) (A).

Scheme 2. The processes of synthesis of ligands H_2L^1 and H_2L^2.

Figure 1. ORTEP representation of H_2L^1.

Figure 2. ^{7}Li NMR spectra of 0.01 M solution of (A) $LiClO_4$ and (B) $Mn(ClO_4)_2$ in acetonitrile at various $[H_2L^1]/[M^{n+}]$ mole ratios at 25°C.

Figure 3. ^{7}Li chemical shifts as a function of the $[H_2L^1]/[M^{n+}]$ mole ratio in acetonitrile and methanol in 25°C.

Figure 4. Computer fit of ^{7}Li chemical shift *vs*. $[H_2L^1]/[Zn^{2+}]$ mole ratio in acetonitrile at 25°C in the presence of Zn^{2+}: (×) experimental point; (o) calculated point; (=) experimental and calculated points are the same within the resolution of the plots.

Figure 5. The viability results of (a) fibroblasts, (b) A2780 and (c) PC3 cells treated with different complexes (12.5-100 μg/ml). The viability was determined by MTT assay after 24 h exposure as described in material and methods. Data are expressed as the mean ±SEM of the three separate experiments.

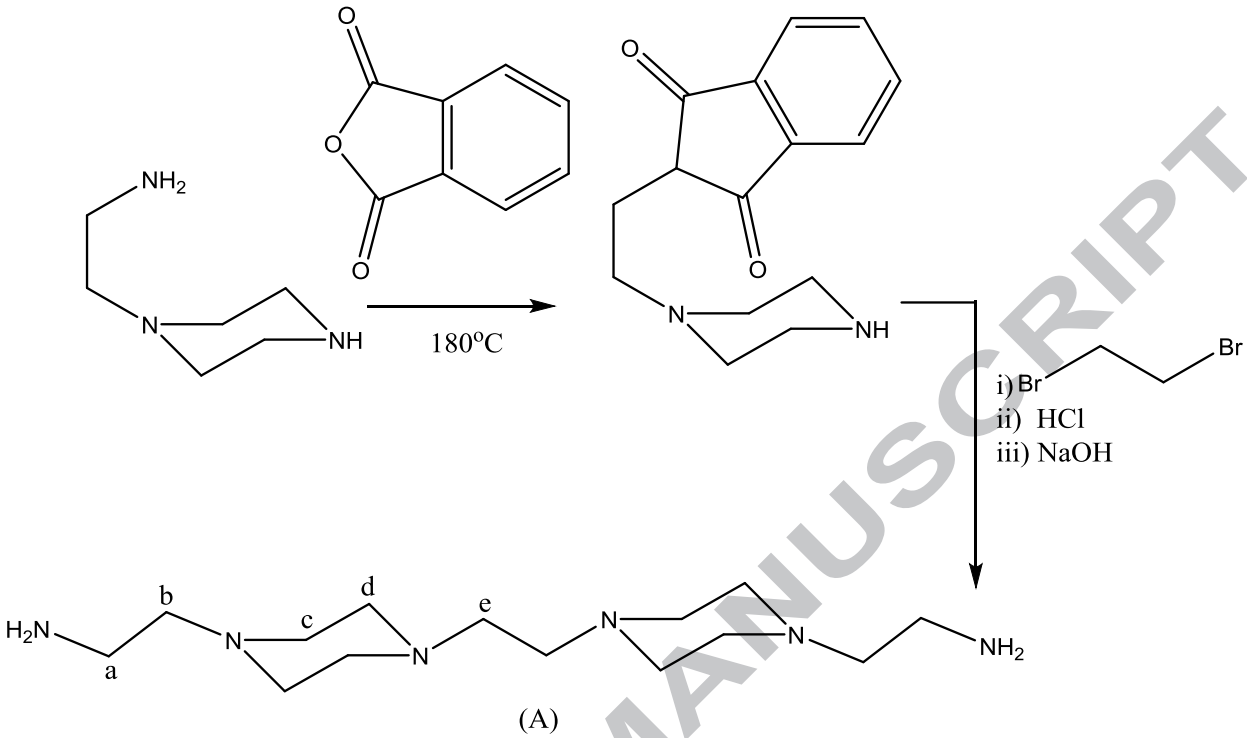

(A)

Scheme 1. The processes of synthesis of 2,2'-(ethane-1,2-diylbis(piperazine-4,1-diyl))bis(ethan-1-amine) (A).

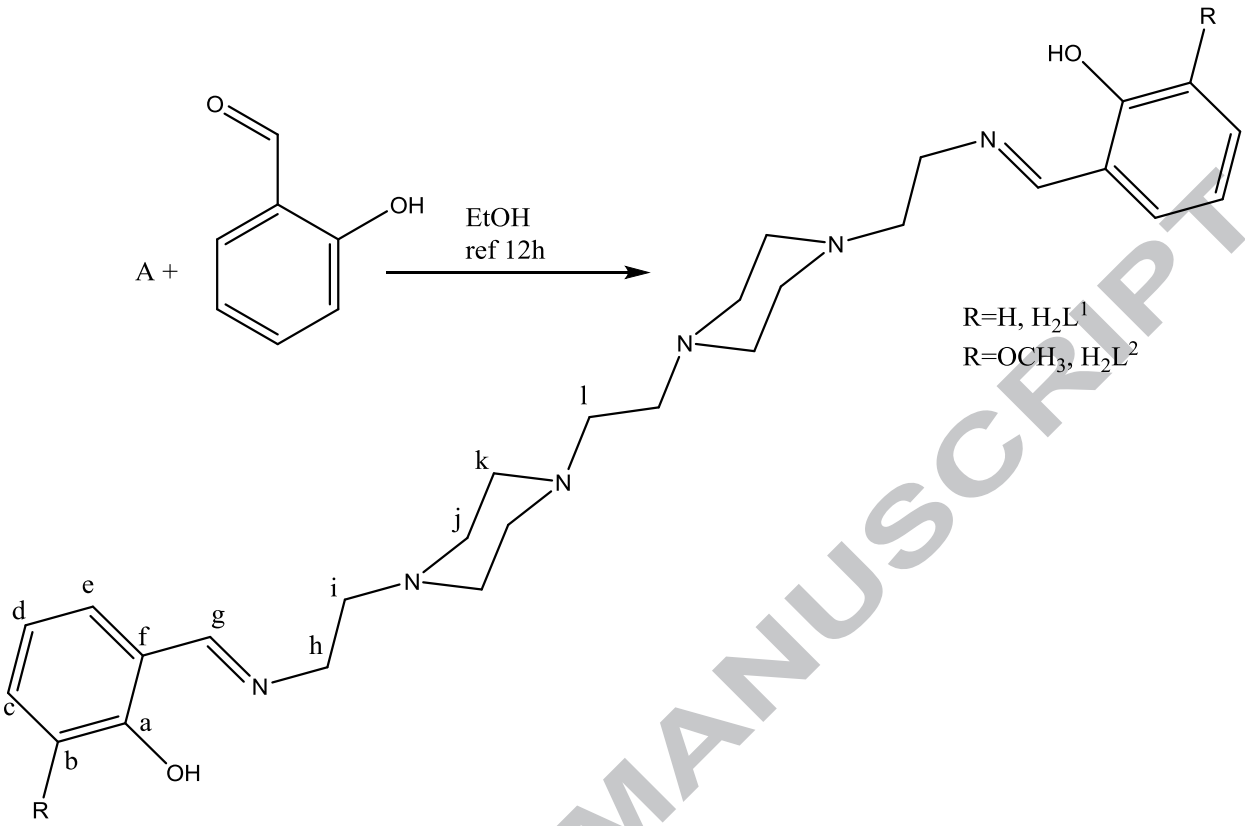

Scheme 2. The processes of synthesis of ligands H_2L^1 and H_2L^2, along with NMR letters.

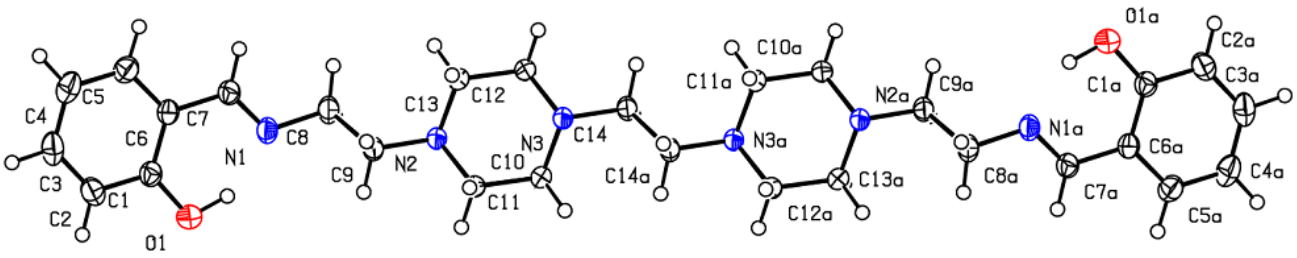

Fig. 1. ORTEP representation of H_2L^1.

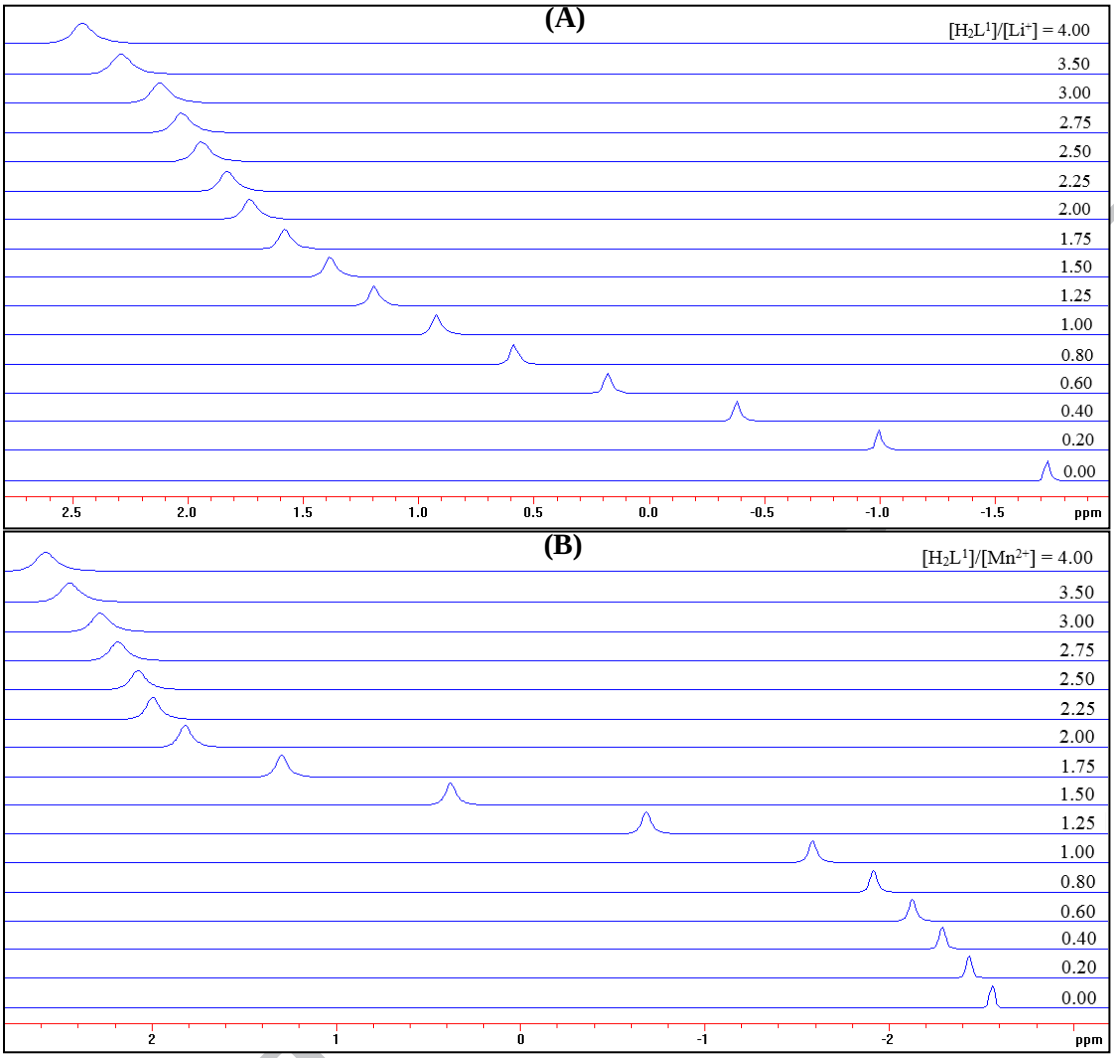

Fig. 2. ^{7}Li NMR spectra of 0.01 M solution of (A) $LiClO_4$ and (B) $Mn(ClO_4)_2$ in acetonitrile at various $[H_2L^1]/[M^{n+}]$ mole ratios at 25°C.

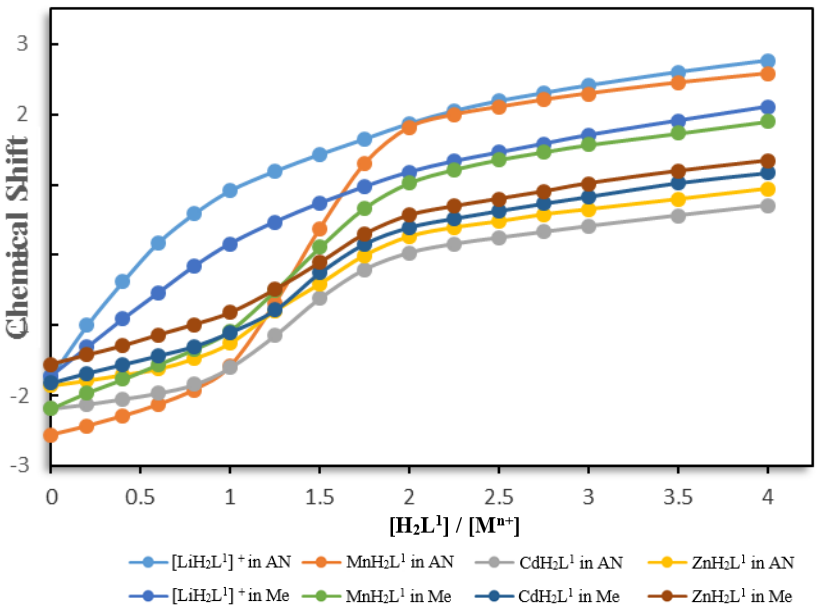

Fig. 3. ^{7}Li chemical shifts as a function of the $[H_2L^1]/[M^{n+}]$ mole ratio in acetonitrile and methanol in 25°C.

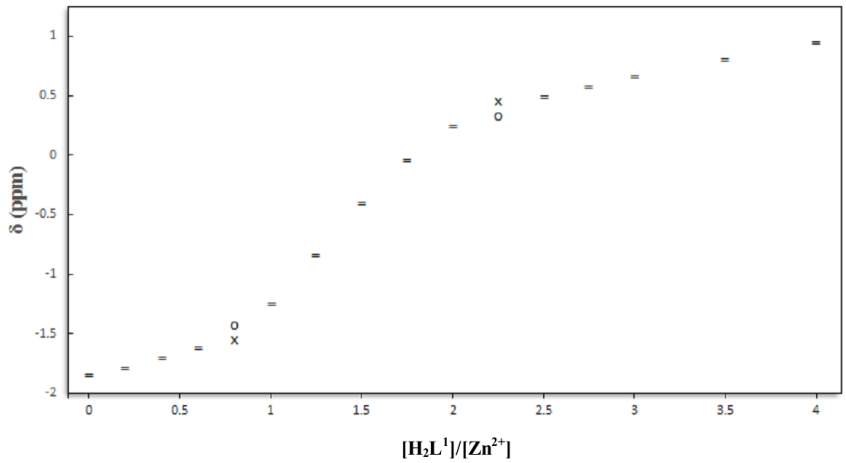

Fig. 4. Computer fit of ^{7}Li chemical shift *vs*. $[H_2L^1]/[Zn^{2+}]$ mole ratio in acetonitrile at 25°C in the presence of Zn^{2+}: (×) experimental point; (o) calculated point; (=) experimental and calculated points are the same within the resolution of the plots.

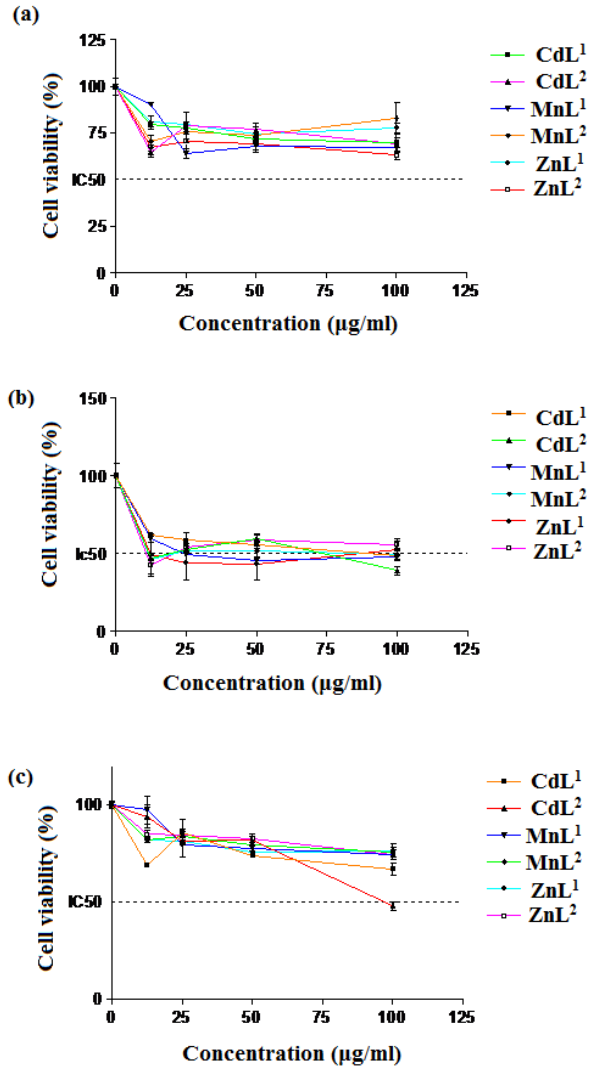

Fig. 5. The viability results of (a) fibroblasts, (b) A2780 and (c) PC3 cells treated with different complexes (12.5-100 µg/ml). The viability was determined by MTT assay after 24 h exposure as described in material and methods. Data are expressed as the mean ±SEM of the three separate experiments.

Graphical abstract

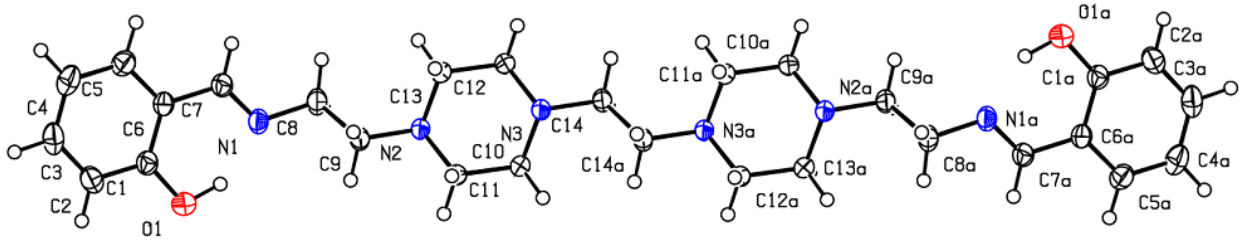

Two new symmetrical Schiff base ligands were derived from condensation of new synthesized polyamine (A) and 2-Hydroxybenzaldehyde (H_2L^1) or 2-hydroxy-3-methoxybenzaldhyde (H_2L^2). Six macroacylic Schiff base complexes were prepared by direct reaction of H_2L^1 or H_2L^2 and Mn(II), Zn(II) and Cd(II) metal ions in equimolar ratios. The crystal structure of H_2L^1 was confirmed by single crystal X-ray analysis. A competitive ^{7}Li NMR manner was used to probe the complexation of Mn^{2+}, $Zn^{2+}$and Cd^{2+} ions with (H_2L^1) and (H_2L^2) in the same solvent systems. Cytotoxic and antibacterial properties of complexes were also investigated.